Ecological Indicators 150 (2023) 110192

Contents lists available at ScienceDirect

Ecological Indicators

journal homepage: www.elsevier.com/locate/ecolind

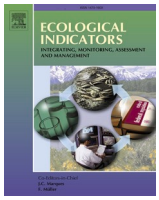

Original Articles

Influences of anthropogenic acids on carbonate weathering and CO_2 sink in an agricultural karst wetland (South China)

Jun Li [a], Hao Xie [b], Jianhong Li [b], Guoli Yang [a], Yincai Xie [b], Jiawei Wang [a], Changsong Zhou [b], Shengzhang Zou [b,*]

[a] Hebei Key Laboratory of Water Quality Engineering and Comprehensive Utilization of Water Resources, Hebei University of Architecture, Zhangjiakou 075000, China
[b] Key Laboratory of Karst Dynamics, MNR&GZAR, Institute of Karst Geology, CAGS, Guilin 541004, China

ARTICLE INFO

Keywords:
Anthropogenic acids
Stable isotope
Carbonate weathering
CO_2 sink
Karst wetland

ABSTRACT

Carbonate minerals are the largest carbon (C) reservoir on earth. Quantitative assessment of carbonate weathering and CO_2 sink flux caused by anthropogenic acids in karst wetland regions is imperative to improve understanding of the hydrogeochemical evolution and global C cycle in karst ecosystem. In this study, a typical field observation was conducted in the Huixian karst wetland (HKW) in South China. The hydrogeochemical and isotopic ($\delta^{15}N\text{-}NO_3^-$, $\delta^{18}O\text{-}NO_3^-$, and $\delta^{13}C_{DIC}$) analyses combined with the MixSIAR model and stoichiometric coefficients were used to quantitatively estimate the influence of H_2CO_3, HNO_3 and H_2SO_4 on carbonate weathering and CO_2 sink flux. The results obtained showed that anthropogenic HNO_3 and H_2SO_4 affect carbonate weathering in the HKW, evidenced by the significant correlations between hydrogeochemical parameters and $\delta^{13}C_{DIC}$ value. The quantitative results showed high contributions of HNO_3 and H_2SO_4 to carbonate weathering in karst groundwater, with contribution ratio values of 20.91 ± 19.29 and 21.69 ± 26.88%, respectively. Besides karst water over-exploitation, this finding suggested that these anthropogenic acids were also an important cause of a decrease in ecological water levels, resulting in the shortage of karst water resource and degradation of wetland ecosystem. Moreover, the involvement of anthropogenic acids in the natural chemical weathering has significantly decreased the CO_2 sink flux by 11.23 ± 7.94 and 41.60 ± 30.24% for surface water and groundwater, respectively, thereby potentially affecting the karst C cycle and global climate change. This present study provided an integrated quantitative approach for estimating the influence of H_2CO_3, HNO_3, and H_2SO_4 on carbonate weathering and CO_2 sink in karst wetland regions. Our study highlighted that the effects of anthropogenic acids on carbonate weathering need to be considered in future studies on the restoration of wetland ecosystems, particularly in intensive agricultural study areas.

1. Introduction

Chemical weathering is a key process of karst evolution, affecting the hydrogeochemical evolution and global carbon (C) cycle in karst ecosystems (Martin, 2017; Xie et al., 2021). Over geological time scales, chemical weathering has little effect on the global C, as atmospheric CO_2 is consumed by carbonate dissolution and then returns to the atmosphere following carbonate precipitation (Berner and Kothavala, 2001; Liu and Han, 2020). However, previous studies have pointed out a considerable amount of the consumed CO_2 via carbonate weathering, accounting for about 43% of global forest C sink (Liu, 2012; Huang et al., 2014). Hence, this natural C sink proportion should be not ignored on short time scales (i.e., 100–100,000 years; Xie et al., 2021). Karst region is known as one of the ecological fragile regions worldwide due to the thin surface soil layer and well-developed karst system (Li et al., 2023). Hence, the karst ecosystem has been affected by intensive anthropogenic activities (e.g., agricultural and mining activities; Perrin et al., 2008; Huang et al., 2017). Indeed, previous studies have shown that anthropogenic acids (e.g., HNO_3 and H_2SO_4) have been involved in carbonate dissolution in karst areas (Zhang et al., 2020; Zhao et al., 2021). Therefore, the involvement of anthropogenic acids in carbonate weathering should be considered on hydrogeochemical evolution and the global C cycle in karst ecosystems.

The H_2CO_3 is produced by the chemical reaction of CO_2 from the atmosphere and/or soil with H_2O. Half of the involved C amount in the natural process of carbonate weathering is derived from the atmosphere

* Corresponding author.
E-mail address: zshengzhang@mail.cgs.gov.cn (S. Zou).

https://doi.org/10.1016/j.ecolind.2023.110192
Received 3 January 2023; Received in revised form 28 February 2023; Accepted 26 March 2023
Available online 4 April 2023

and/or soil CO_2, while the remaining part is derived from carbonate minerals ($Ca_xMg_{1-x}CO_3 + H_2O + CO_2 \rightarrow xCa^{2+} + (1-x)Mg^{2+} + 2HCO_3^-$, Eq. (1); Martin, 2017; Jiang et al., 2013). However, carbonate minerals may be also dissolved by anthropogenic acids from human activities inputs (e.g., HNO_3 and H_2SO_4; Raymond et al., 2008; Cartwright, 2010). The disturbed processes of chemical weathering do not require exogenous CO_2, thus all the HCO_3^- generated is derived from carbonate minerals ($Ca_xMg_{1-x}CO_3 + HNO_3 \rightarrow xCa^{2+} + (1-x)Mg^{2+} + HCO_3^- + NO_3^-$ (Eq. (2)) and $2Ca_xMg_{1-x}CO_3 + H_2SO_4 \rightarrow 2xCa^{2+} + 2(1-x)Mg^{2+} + 2HCO_3^- + SO_4^{2-}$ (Eq. (3)); Huang et al., 2017 and Xie et al., 2021). Thus, anthropogenic HNO_3 and H_2SO_4 involved in carbonate weathering may have several effects on the karst ecosystems. Fist, disturbed karst hydrogeochemical processes can result in a significant decrease in the CO_2 sink flux (Perrin et al., 2008), which affects global climate change; Second, the relatively strong anthropogenic acids can accelerate the carbonate dissolution and karst development (Waele et al., 2016), thereby decreasing ecological water levels and deteriorating karst ecosystems; Third, the anthropogenic acids may increase NO_3^- and SO_4^{2-} concentrations in karst groundwater, resulting in karst groundwater pollution (Jiang, 2013). In fact, the carbonate dissolution is dominated by H_2CO_3 in most karst agricultural areas, accompanied by a certain proportion of HNO_3 and H_2SO_4 ($(a_1 + a_2 + 2a_3)Ca_xMg_{1-x}CO_3 + a_1HCO_3 + a_2HNO_3 + a_3H_2SO_4 \rightarrow (a_1 + a_2 + 2a_3)xCa^{2+} + (a_1 + a_2 + 2a_3)(1-x)Mg^{2+} + (2a_1 + a_2 + 2a_3)HCO_3^- + a_2NO_3^- + a_3SO_4^{2-}$ (Eq. (4); Huang et al., 2017)). The higher contribution rate of anthropogenic acids to carbonate dissolution is related to their greater influences on the karst ecosystems. Therefore, it is essential to estimate the proportional contributions of anthropogenic acids to carbonate dissolution.

Hydrogeochemical processes lead to distinctive isotopic fingerprints, providing useful insights for understanding the sources of anthropogenic acid pollution and chemical weathering processes (Ren et al., 2022). For instance, synthetic fertilizers exhibit low nitrate isotopes values, while animal waste and domestic sewage present high nitrate isotopes values (Xue et al., 2009), making it possible to quantify the contribution of different NO_3^- sources in karst water. Moreover, high HCO_3^- concentrations from the atmosphere and/or soil CO_2 can result in low $\delta^{13}C_{DIC}$ values, while high HCO_3^- concentrations from carbonate minerals result in high $\delta^{13}C_{DIC}$ values in karst water (Ren et al., 2022). Therefore, the involvement of anthropogenic acids in carbonate weathering is evidenced by $\delta^{13}C_{DIC}$ fingerprints (Wachniew, 2006). Indeed, multiple stable isotopes have been widely used in karst hydrogeochemical studies, including pollution source and carbonate weathering (Xue et al., 2009; Jiang, 2013).

The wetland ecosystems are known as the “kidneys of the earth”, particularly karst wetland ecosystems that exhibit rapid water and C exchanges. Numerous studies have investigated the contributions of anthropogenic acids to carbonate weathering in karst areas, focusing mainly on chemical weathering and dissolved inorganic carbon (DIC) flux (Zhang et al., 2020; Xie et al., 2021). However, although karst wetlands are of great significance for the hydrogeochemical evolution and C cycle in karst ecosystems, few studies on the contribution estimation of anthropogenic acids to carbonate weathering and CO_2 sink, and discussion of adverse effects of this disturbed process on karst ecosystems in karst wetlands have been carried out. In this study, a typical field observation was conducted in the Huixian karst wetland (HKW), which has been mainly polluted by NO_3^- and SO_4^{2-} in karst water (Li et al, 2021). We hypothesized that: (i) a considerable portion of NO_3^- and SO_4^{2-} in karst water would be produced from anthropogenic acids (i.e., HNO_3 and H_2SO_4) in the HKW, (ii) the anthropogenic acids would be involved in the natural carbonate weathering, and (iii) the corresponding perturbation process would decrease the ecological water level and reduce the CO_2 sink flux.

2. Materials and methods

2.1. Study area

The HKW is located in the core area of the East Asian karst area, which is one of the three largest karst areas worldwide. The study area (longitudes 110°09′E-110°17′E and latitudes 25°05′N-25°09′N) is the main area of HKW, covering an area of about 58 km^2 (Fig. 1). The climate in the study area is characterized by a mid-subtropical monsoon climate, with a mean annual temperature and mean annual precipitation of 19.2 ℃ and 1863.2 mm, respectively (Li et al., 2022). Most regional altitude ranges from 148 to 155 m. Due to strong rock-water interaction, the northern topography of the HKW is characterized by peak cluster depressions, with a relative decrease gradient range of 40–150 m, while the central and southern parts of the study area are characterized by flat topography, where large numbers of agricultural and residential lands are found.

The underlying karst geology consists mainly of the Lower Carboniferous (C_1), Upper Devonian (D_3), and Middle Devonian (D_2), which are mainly composed of limestone, dolomite, and dolomitic limestone intercalated with some detrital rocks (Li et al., 2023). The Guiguliu River and Mudong Lake are the main karst surface rivers in the study area. The surface water area has shrunk in recent decades due to the decrease in groundwater levels. Furthermore, the shortage of karst water resources has induced a series of karst ecological environmental problems, such as wetland degradation and biodiversity reduction (Zou et al., 2019). The thin surface soil layer and well-developed underground karst system lead to a weak resistance to surface pollutants, therefore, the karst ecological environment system is sensitive to surface agricultural and mining activities and has a relatively high pollution risk in the HKW. Furthermore, Li et al. (2021) has revealed that the karst water was adversely affected by surface acid pollutants (e.g., NO_3^- and SO_4^{2-}) in the HKW.

2.2. Sampling and analytical methods

Representative monitoring sites were selected in the HKW in this study. In total, 10 surface water (SW01-SW10, from rivers and lakes) and 13 groundwater (GW01-GW13, from wells and underground rivers) samples were collected from the HKW in August 2018 (Fig. 1). Sample collection, storage, and transportation processes were strictly conducted based on Groundwater Quality Standards (GB/T14848–2017) (Standardization Administration, 2017). During the sampling period, large amounts of synthetic fertilizers were applied in farmlands. In addition, the pyrite slag in the northern part of the study area was frequently leached by heavy rainfall, resulting in karst groundwater pollution by anthropogenic acid pollutants, thereby contributing to water–rock interaction. Therefore, the collected water samples can provide further insight into the quantification of chemical weathering and CO_2 sink associated with anthropogenic HNO_3 and H_2SO_4.

In this study, pH, temperature (T), dissolved oxygen (DO), electrical conductivity (EC), and total dissolved solids (TDS) of water were measured in-situ using HACH HQ40d multiparameter instrument (United States), while HCO_3^- was measured in-situ using the Aquamerck Alkalinity test kits (Germany). All water samples were filtered through 0.45-μm and 0.22-μm pore-size acetate cellulose membranes for hydrogeochemical and isotopic analyses, respectively. The concentrations of cations (K^+, Na^+, Ca^{2+}, and Mg^{2+}) and anions (Cl^-, SO_4^{2-}, and F^-) were analyzed using Dionex ICS-1500 ion chromatograph (United States) and Metrohm MIC ion chromatograph (Switzerland), respectively. The NO_3^-, NO_2^-, and NH_4^+ concentrations were analyzed using Perkin-Elmer Lambda 35 spectrophotometry (United States). In addition, analytical precision was assessed using standard reference materials and regent blank during the entire analytical process. Standard deviation values less than 5% were considered acceptable.

The details of stable isotopes measurements were presented in pre-

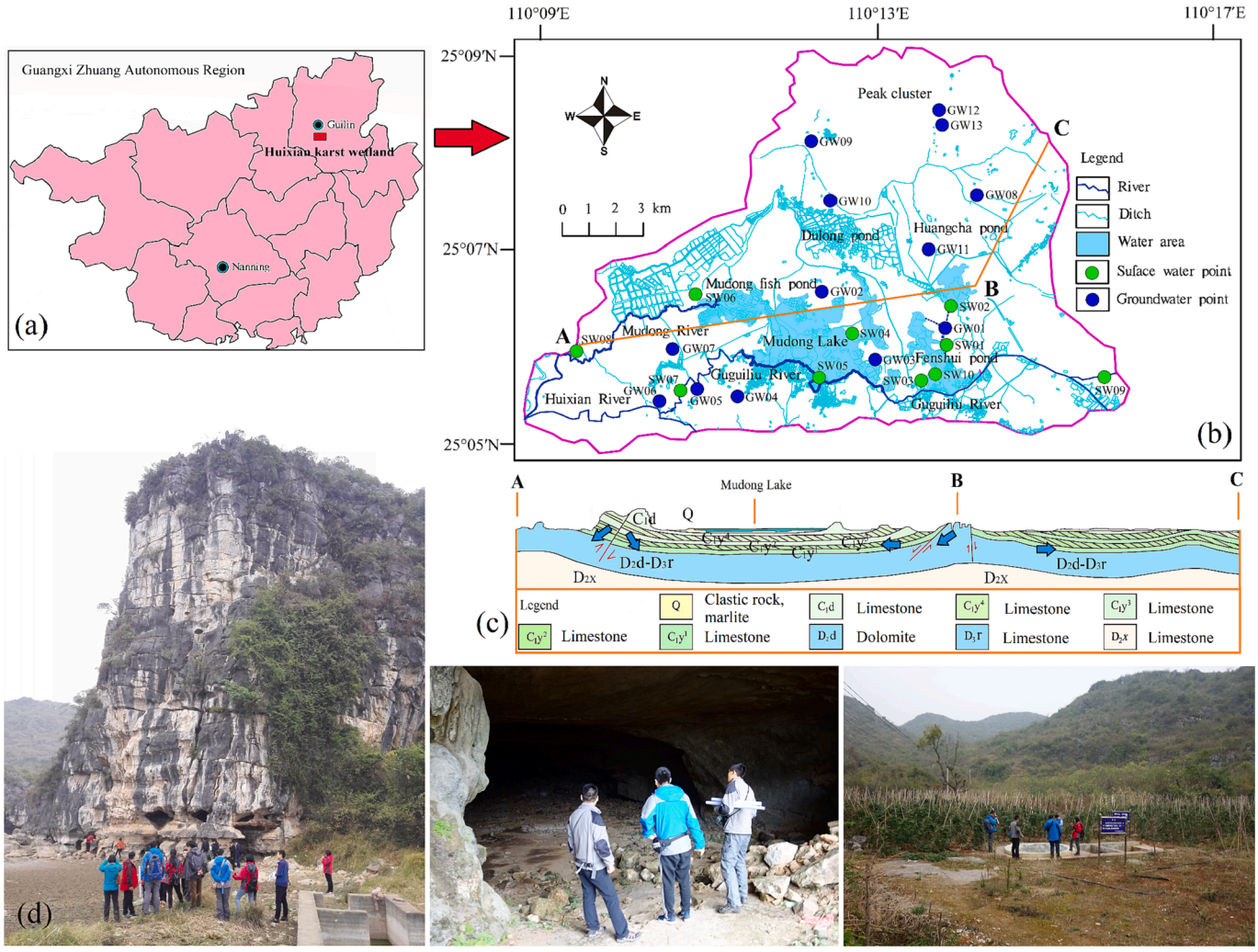

Fig. 1. (a) Location map of the Huixian karst wetland in Guangxi Zhuang Autonomous Region; (b) sampling sites, river networks, (c) lithology and sectional view of the study area; (d) pictures showing karst development, underground rivers, and agricultural land in the study area.

vious study (Li et al., 2023). In short, the $\delta^{15}N\text{-}NO_3^-$ and $\delta^{18}O\text{-}NO_3^-$ values were determined using ion-exchange methods combined with Finnigan MAT-253 mass spectrometer (United States) and online Flash Elemental Analyzer (Silva et al., 2000). The international calibration standards (USGS32 and USGS34 for $\delta^{15}N\text{-}NO_3^-$, and USGS34 and USGS35 for $\delta^{18}O\text{-}NO_3^-$) were applied during measurements. The $\delta^{13}C_{DIC}$ were acidified by phosphoric acid, and then determined by GasBench-IRMS (USA) (Han et al., 2010). The internal (GBW04416 and GBW04417) and international (NBS19) standards were employed during the measurement process of $\delta^{13}C_{DIC}$. The analytical precisions of $\delta^{15}N\text{-}NO_3^-$, $\delta^{18}O\text{-}NO_3^-$, and $\delta^{13}C_{DIC}$ were lower than ± 0.3, ±0.8, and ± 0.2‰, respectively. The isotopic compositions were expressed in delta (δ) with respect to the Vienna-Standard Mean Ocean Water (V-SMOW) for O, atmospheric N (N_2) for N, and Vienna-Pee Dee Belemnite (V-PDB) for C, according to the following formulas:

$$\delta(‰) = \left(R_{sample}/R_{standard} - 1\right) \times 1000 \quad (5)$$

Where R_{sample} and $R_{standard}$ are the $^{18}O/^{16}O$, $^{15}N/^{14}N$, and $^{13}C/^{12}C$ ratios of samples and standards, respectively.

2.3. Calculation of carbonate weathering and CO_2 sink

Xie et al. (2021) has revealed significantly lower Ca^{2+} and Mg^{2+} concentrations in rainwater than those in karst water in Guangxi Province. Furthermore, Li et al. (2021) showed mineral dissolution is the main source of Ca^{2+} and Mg^{2+} in karst water of the HKW. Therefore, it was assumed that all Ca^{2+}, Mg^{2+}, and HCO_3^- in karst water are derived from carbonate weathering by H_2CO_3, HNO_3, and H_2SO_4 in this study. In addition, we assumed that carbonate minerals were simultaneously dissolved by a_1 mmol/L H_2CO_3, a_2 mmol/L HNO_3, and a_3 mmol/L H_2SO_4 according to Eq. (4). Hence, Ca^{2+}, Mg^{2+}, and HCO_3^- concentrations were determined according to following equations:

$$c\left(Ca^{2+} + Mg^{2+}\right)_{carbonatedissolution} = (a_1 + a_2 + 2a_3) \quad (6)$$

$$c\left(HCO_3^-\right)_{carbonate\ dissolution} = (2a_1 + a_2 + 2a_3) \quad (7)$$

The value of a_1 was calculated using the following formula (Huang et al., 2017):

$$a_1 = Eq.(7) - Eq.(6) = c\left(HCO_3^-\right)_{carbonate\ dissolution} - c\left(Ca^{2+} + Mg^{2+}\right)_{carbonate\ dissolution} \quad (8)$$

The proportional contributions of dissolved carbonate by H_2CO_3 to the total Ca^{2+}+Mg^{2+} (w_1) and HCO_3^- (s_1) concentrations were determined according to the following formulas (Xie et al., 2021):

$$w_1 = a_1/c\left(Ca^{2+} + Mg^{2+}\right)_{carbonate\ dissolution} \quad (9)$$

$$s_1 = 2a_1/c\left(HCO_3^-\right)_{carbonate\ dissolution} \quad (10)$$

The NH_4^+ can be transformed into HNO_3 under the microbial

nitrification process (Zhang et al., 2020). For example, NHF (e.g., CO$(HN_2)_2$, NH_4NO_3, NH_4Cl, et al.) is oxidized by autotrophic bacteria, such as *Nitrosomonas* and *Nitrobacter*, resulting in NO_3^- and H^+ in karst water (Perrin et al., 2008). Therefore, estimating NO_3^- sources is a key step in HNO_3 quantification in karst water. Li et al. (2023) has shown that atmospheric deposition (AD), NH_4^+-synthetic fertilizer (NHF), NO_3^--synthetic fertilizer (NOF), soil organic nitrogen (SN), and manure and domestic sewage (MS) are the main sources of NO_3^- in the HKW. The contribution rates (*CR*) of AD, NHF, NOF, SN, and MS to karst water NO_3^- can be determined using the MixSIAR model combined with multiple isotopes. Hence, HNO_3 concentration involved in chemical weathering can be determined according to the following formulas (Zhang et al., 2020):

$$a_2 = c\left(NO_3^-\right) \times \left(CR_{AD} + CR_{NHF} + CR_{SN} + CR_{MS}\right) \quad (11)$$

According to Eq. (6), the involved H_2SO_4 concentration in chemical weathering was calculated using the following formula:

$$a_3 = \left[c\left(Ca^{2+} + Mg^{2+}\right)_{carbonatedissolution} - a_1 - a_2\right]/2 \quad (12)$$

Therefore, the proportional contributions of carbonate weathering by HNO_3 and H_2SO_4 to the total (Ca^{2+}+Mg^{2+}) (w_2 and w_3) and HCO_3^- (s_2 and s_3) concentrations can be estimated according to the following formulas:

$$w_2 = a_2/c\left(Ca^{2+} + Mg^{2+}\right)_{carbonatedissolution} \quad (13)$$

$$s_2 = a_2/c\left(HCO_3^-\right)_{carbonatedissolution} \quad (14)$$

$$w_3 = 2a_3/c\left(Ca^{2+} + Mg^{2+}\right)_{carbonatedissolution} \quad (15)$$

$$s_3 = 2a_3/c(HCO_3^-)_{carbonatedissolution} \quad (16)$$

According to Eqs. (1–3), 1 mmol/L carbonate minerals dissolved by H_2CO_3 consume 1 mmol/L CO_2 and 1 mmol/L H_2O and produce 2 mmol/L HCO_3^-, whereas 1 mmol/L carbonate minerals dissolved by HNO_3 and H_2SO_4 require no CO_2 consumption and produce only 1 mmol/L HCO_3^-. However, if anthropogenic HNO_3 and H_2SO_4 are involved in carbonate weathering, the calculation is still based on the natural dissolution process, which is likely to overestimate the CO_2 sink flux. The over-estimation proportion of CO_2 sink (OP_{CO2}) can, therefore, be determined according to the following formula:

$$OP_{CO2} = [1 - a_1/(a_1 + a_2 + 2a_3)] = (a_2 + 2a_3)/c\left(Ca^{2+} + Mg^{2+}\right)_{carbonate\ dissolution} \quad (17)$$

3. Results

3.1. Hydrogeochemical compositions

The obtained hydrogeochemical composition results of all karst water samples are reported in Table 1. The pH values of SW and GW ranged from 7.15 to 7.57 and 6.69 to 7.50, with mean values of 7.41 and 7.33, respectively, indicating neutral to slightly alkaline SW and GW in the HKW. In fact, 95.65% of the collected water samples exhibited pH values over 7, indicating carbonate weathering (Xie et al., 2021). The mean T value of GW was relatively lower than those of SW, showing T values of 27.6 ± 2.12 and 30.2 ± 1.18 ℃, respectively. The TDS presented a higher mean value in GW than SW of 406 ± 506 and 188 ± 26.0 mg/L, respectively, which might be due to the stronger influence of chemical weathering in karst aquifers than that in surface water. The mean values of total cationic ($TZ^+ = K^+ + Na^+ + 2Ca^{2+} + 2\ Mg^{2+}$, Eq. (18)) and total anionic ($TZ^- = Cl^- + 2SO_4^{2-} + HCO_3^- + NO_3^-$, Eq. (19)) charges were 3.61 ± 0.53 and 3.49 ± 0.48 meq/L for SW, and 6.91 ± 8.31 and 6.97 ± 8.14 meq/L for GW, respectively. Furthermore, the values of normalized inorganic charge balance ($NICB = (TZ^+ - TZ^-) \times 100\% / (TZ^+ + TZ^-)$, Eq. (20)) ranged from 0.38 to 2.55% and 0.49 to 2.33% for SW and GW, respectively, showing that all values were close to zero, thereby suggesting a small contribution of organic complex matters to the charge balance and insignificant analytical uncertainty in this study.

The hydrochemical facies types and dominant ions were determined in this study using the Piper diagram (Fig. S1). The results showed that about 95.65% of the collected water samples were close to the diagram part of Ca^{2+} and HCO_3^-, indicating that the HCO_3-Ca type was the main hydrochemical facies type of water in the HKW. Therefore, the hydrogeochemical process in the study area was mainly controlled by calcite weathering. The saturation index of calcite (SIc) of SW and GW varied from –0.21 to 0.30 and –1.29 to 0.39, with average values of 0.05 and 0.04 for GW, respectively (Table 1), suggesting that saturation or slight over-saturation with respect to calcite were reached at most sampling

Table 1
Descriptive statistics of hydrogeochemical and stable isotopic compositions in SW and GW of the HKW.

Parameters	Units	Surface water (n = 10)					Groundwater (n = 13)				
		Max	Min	Mean	SD	CV	Max	Min	Mean	SD	CV
pH		7.57	7.15	7.41	0.14	0.02	7.50	6.96	7.33	0.18	0.02
T	℃	32.4	28.0	30.2	1.18	0.04	32.1	24.6	27.6	2.12	0.08
DO	mg/L	6.54	0.56	4.13	1.72	0.42	7.92	3.71	5.43	1.26	0.23
EC	μS/cm	376	258	318	44.4	0.14	2287	183	586	535	0.91
TDS	mg/L	227	153	188	26.0	0.14	2060	118	406	506	1.25
K^+	mg/L	7.59	2.49	4.62	1.63	0.35	63.8	0.35	13.2	22.2	1.68
Na^+	mg/L	4.74	1.72	2.61	1.01	0.39	21.6	0.87	7.00	6.82	0.97
Ca^{2+}	mg/L	65.2	42.5	53.5	7.16	0.13	269	22.8	85.0	59.0	0.69
Mg^{2+}	mg/L	9.56	4.62	6.82	1.65	0.24	247	1.46	24.1	66.9	2.78
Cl^-	mg/L	10.2	2.96	6.67	2.31	0.35	20.1	2.33	9.56	5.97	0.62
SO_4^{2-}	mg/L	13.0	6.78	8.97	1.97	0.22	1375	6.32	124	376	3.03
HCO_3^-	mg/L	230	153	189	25.4	0.13	258	54.1	203	56.2	0.28
NO_3^-	mg/L	2.00	BDL	0.65	0.82	1.27	117	1.43	34.8	35.0	1.01
NH_4^+	mg/L	13.7	0.12	2.37	4.11	1.73	0.41	BDL	0.06	0.11	1.94
F^-	mg/L	0.28	0.08	0.13	0.06	0.47	0.13	BDL	0.07	0.04	0.50
TZ^+	meq/L	4.43	2.91	3.61	0.53	0.15	34.12	1.88	6.91	8.31	1.20
TZ^-	meq/L	4.25	2.84	3.49	0.48	0.14	33.41	1.85	6.75	8.14	1.21
NICB	%	2.55	0.38	1.58	0.69	0.43	2.33	0.49	1.10	0.54	0.49
SIc		0.30	–0.21	0.05	0.20	4.03	0.39	–1.29	0.04	0.42	11.04
pCO_2	ppmv	13,932	5297	8044	2486	0.31	17,660	5248	9584	3943	0.41
$\delta^{15}N\text{-}NO_3^-$	‰	+4.28	–3.53	+1.19	2.78	2.34	+6.41	–4.76	+1.79	3.26	1.83
$\delta^{18}O\text{-}NO_3^-$	‰	+15.9	+1.98	+8.83	4.46	0.51	+17.1	+4.74	+8.75	3.93	0.45
$\delta^{13}C_{DIC}$	‰	–6.22	–11.47	–9.22	1.88	–0.20	–6.93	–13.79	–11.03	2.11	–0.19

Note: Max: maximum; Min: minimum; SD: standard deviation; CV: coefficient of variation; BDL: below detection limit.

points (Liu and Han, 2020). However, the SO_4-Ca·Mg facies type was observed only at GW12 with SO_4^{2-}, Ca^{2+}, and Mg^{2+} concentrations of 1375, 269, and 247 mg/L, respectively. The primary source of SO_4^{2-} pollution was mainly derived from waste residue of pyrite situated in the northern area of HKW, which has been evidenced by the previous study (Li et al., 2021). Furthermore, the sum of milligram equivalent concentrations of Ca^{2+} and Mg^{2+} were over the corresponding HCO_3^- concentrations in most water samples (Fig. 2a), while the cationic excess between Ca^{2+}+Mg^{2+} and HCO_3^- was compensated by NO_3^- and SO_4^{2-} (Fig. 2b). Hence, HNO_3 and H_2SO_4 might be involved in the carbonate weathering processes.

3.2. Isotopic compositions

The $\delta^{15}N$-NO_3^- and $\delta^{18}O$-NO_3^- values ranged from –3.53 to + 4.28‰ and 1.98 to + 15.9‰, with mean values of + 1.19 and + 8.83‰ for SW and from –4.76 to + 6.41‰ and + 4.74 to + 17.1‰, with mean values of + 1.79 and + 8.75‰ for GW (Table 1), respectively. Theoretically, the ^{15}N-NO_3^- and ^{18}O-NO_3^- are more enriched in GW due to the occurrence of microbial chemical processes between surface, vadose, and subsurface. However, SW and GW showed slightly similar $\delta^{15}N$-NO_3^- and $\delta^{18}O$-NO_3^- values as a result of the rapid exchange of waters in the HKW.

The $\delta^{13}C_{DIC}$ values of SW and GW ranged from –11.47 to –6.22‰ and –13.79 to –6.93‰, with mean values of –9.22 and –11.03‰ (Table 1), respectively. The slightly higher mean $\delta^{13}C_{DIC}$ value of SW than that of GW suggests more exchange between the SW DIC and atmosphere and/or soil CO_2.

3.3. Contribution ratios of H_2CO_3, HNO_3, and H_2SO_4 to carbonate weathering and of CO_2 sink flux

The contribution ratios of H_2CO_3, HNO_3, and H_2SO_4 to carbonate weathering and CO_2 sink in the HKW are presented in Table S1. The mean contribution proportions of H_2CO_3 (w_1), HNO_3 (w_2), and H_2SO_4 (w_3) to carbonate weathering were 88.77 ± 7.94, 0.57 ± 0.72, and 10.66 ± 8.02% in SW and 57.50 ± 30.24, 20.91 ± 19.29, and 21.69 ± 26.88% in GW, respectively. The mean contribution proportions in GW were higher than those revealed in SW, suggesting stronger chemical weathering in GW compared with that in SW.

The contribution rates of carbonate minerals dissolved by H_2CO_3 (s_1), HNO_3 (s_2), and H_2SO_4 (s_3) to the total HCO_3^- concentrations were 93.88 ± 4.47, 0.30 ± 0.38 and 5.82 ± 4.52% in SW and 67.78 ± 31.02, 15.18 ± 14.52, and 17.03 ± 25.28% in GW, respectively. Whereas the Op_{co2} was 11.23 ± 7.94% and 42.60 ± 30.24% in SW and GW (Table S1), respectively, suggesting decreases in the karst C sink flux by 11.23% for SW and 42.60% for GW, which may be considerable amounts of karst C sink decreased by anthropogenic acids in chemical weathering processes in the HKW.

4. Discussion

4.1. Principal component analysis

In this study, 10 hydrogeochemical parameters (i.e., K^+, Na^+, Ca^{2+}, Mg^{2+}, Cl^-, SO_4^{2-}, HCO_3^-, NO_3^-, NH_4^+, and F^-) in all samples were considered in the PCA analysis to determine the involvement of anthropogenic acids in the carbonate weathering (Table S2). The PC1, PC2, and PC3 explained 34.54, 30.67, and 17.27% of the total variance, respectively, with a cumulative explained variance (82.48%) of over 75%. The PC1 showed strong positive loadings on Ca^{2+} (0.956), Mg^{2+} (0.853), SO_4^{2-} (0.864), and HCO_3^- (0.537), suggesting strong carbonate weathering. Moreover, the high loading of PC1 on SO_4^{2-} suggested that H_2SO_4 was obviously involved in carbonate weathering (Liu and Han, 2020). PC2 revealed high loadings on K^+ (0.825), Na^+(0.845), Cl^- (0.935), and NO_3^- (0.596), demonstrating the potential impacts of agricultural inputs (synthetic fertilizers and livestock manure) and domestic sewage on karst water. However, the positive loading of PC2 on NO_3^- (0.596) was slightly lower than that of PC1 (0.475), suggesting that HNO_3 was likely to participate in chemical weathering (Ren et al., 2022). PC3 revealed high positive loadings mainly on NH_4^+ (0.865) and F^- (0.736), indicating low concentrations of ions in karst water. Overall, besides H_2CO_3, the PCA results indicated that HNO_3 and H_2SO_4 played also important roles in the carbonate dissolution process in the HKW.

4.2. Involvement of H_2CO_3, HNO_3, and H_2SO_4 in carbonate weathering

4.2.1. Hydrogeochemical indicators

The hydrogeochemical process in the HKW is primarily controlled by rock-water interaction (Li et al., 2021). According to Fig. 3a, most of the sampling points were plotted in the calcite dissolution zone, which is consistent with large amounts of calcite distributed in the HKW (Fig. 1). Since the HKW is far from the South China Sea, the concentrations of Ca^{2+} and Mg^{2+} in precipitation (10^{-2}–10^{-1} mg/L) were 2–4 orders of magnitude lower than those observed in karst water, especially in GW. In addition, HCO_3^- concentrations in precipitation were below the detection limit (BDL) in Guangxi Province (Zeng et al., 2020; Xie et al., 2021). Therefore, precipitation contributes little to karst water Ca^{2+}, Mg^{2+}, and HCO_3^- in the HKW.

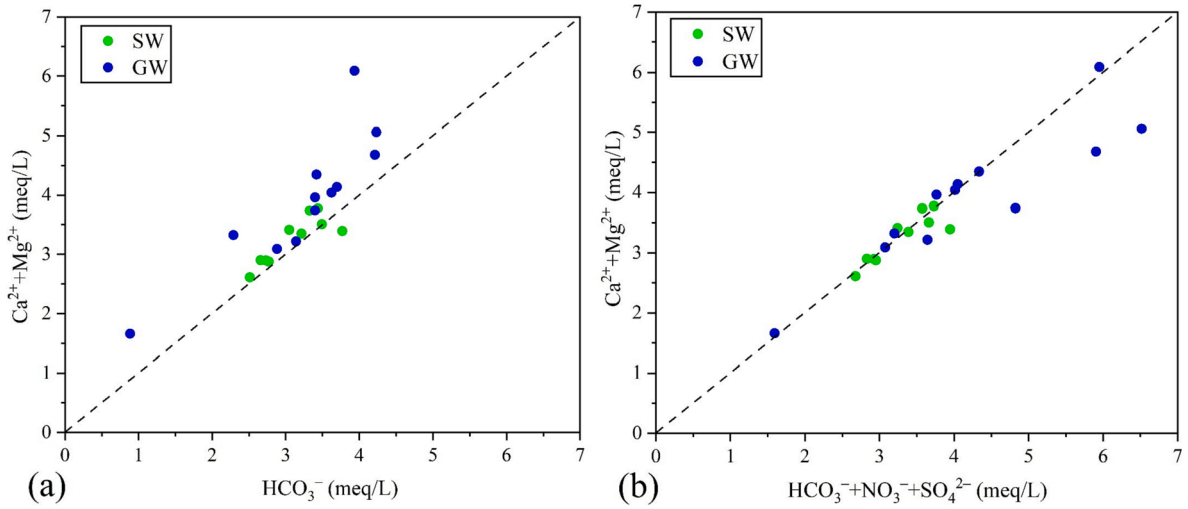

Fig. 2. Co-variation of (a) HCO_3^- and Ca^{2+}+Mg^{2+}, and (b) HCO_3^-+NO_3^-+SO_4^{2-} and Ca^{2+}+Mg^{2+} in SW and GW of the HKW.

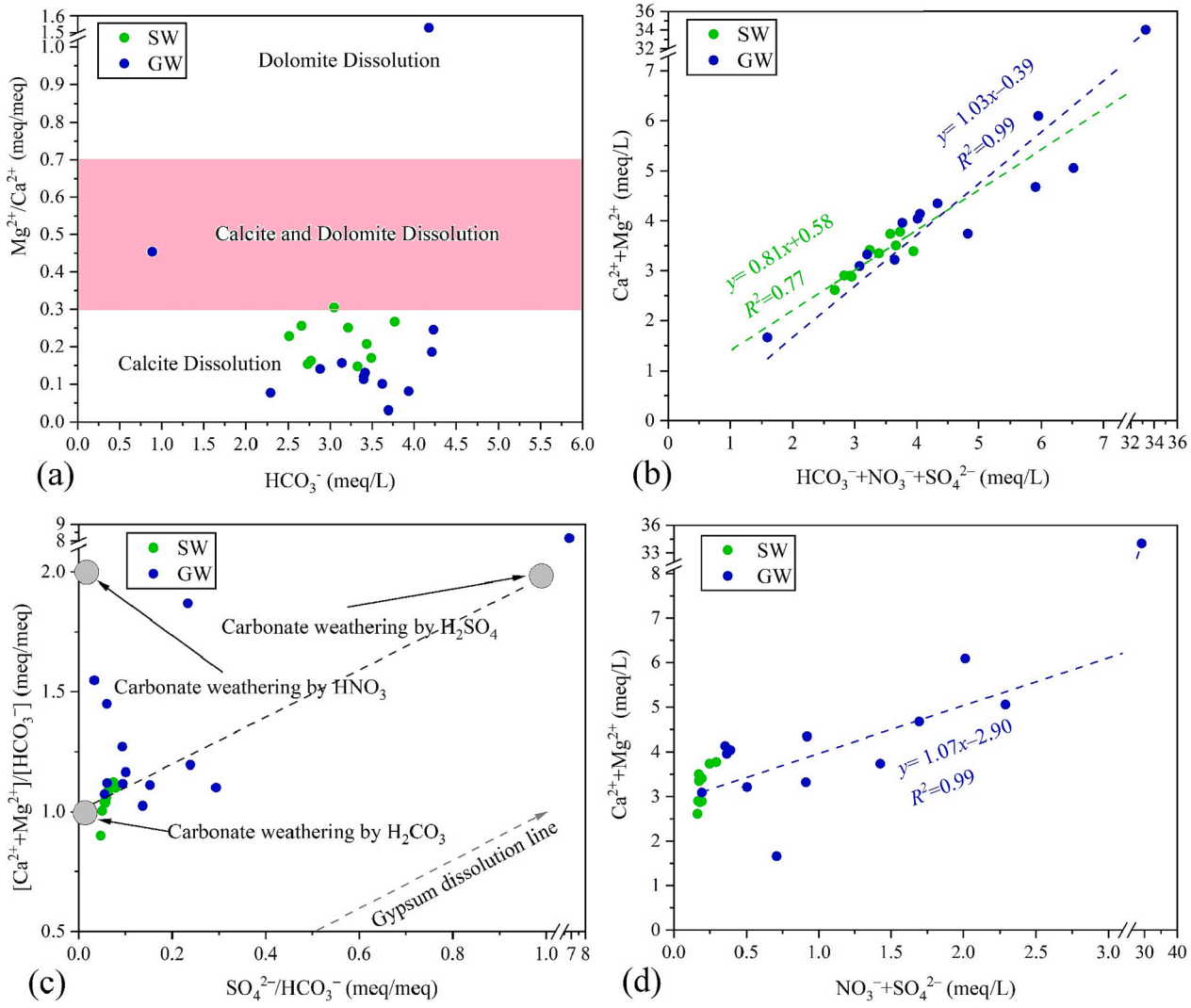

Fig. 3. Mixing diagrams using (a) HCO_3^- versus Mg^{2+}/Ca^{2+}, (b) $HCO_3^-+NO_3^-+SO_4^{2-}$ versus $Ca^{2+}+Mg^{2+}$, (c) SO_4^{2-}/HCO_3^- versus $[Ca^{2+}+Mg^{2+}]/[HCO_3^-]$, and (d) $NO_3^-+SO_4^{2-}$ versus $Ca^{2+}+Mg^{2+}$ in all samples collected from the HKW.

According to Eq. (1), if carbonate minerals are only dissolved by H_2CO_3, the $Ca^{2+}+Mg^{2+}$ milliequivalent should be equal to HCO_3^- in karst water. The $[Ca^{2+}+Mg^{2+}]/[HCO_3^-]_{meq/meq}$ ratio values were, in fact, over 1 in karst water (Fig. 2a), indicating that anthropogenic acids were involved in the carbonate dissolution process (Huang et al., 2017). Theoretically, when the carbonate weathering is dominated by H_2CO_3, HNO_3, and H_2SO_4, the ratios of $[Ca^{2+}+Mg^{2+}]/[HCO_3^-+NO_3^-+SO_4^{2-}]_{meq/meq}$ should be equal to 1 (Xie et al., 2021). According to Fig. 3b, the milliequivalent ratios were close to 1 in both SW (0.81) and GW (1.03), showing very good regression ($R^2 = 0.77$ for SW and $R^2 = 0.99$ for GW), thereby implying that carbonate minerals were also dissolved by HNO_3 and H_2SO_4, with a certain contribution ratio. Moreover, three end members associated with carbonate weathering by H_2CO_3, HNO_3, and H_2SO_4 are shown in Fig. 3c. The carbonate mineral dissolutions by H_2CO_3, HNO_3, and H_2SO_4 can result in $[Ca^{2+}+Mg^{2+}]/[HCO_3^-]_{meq/meq}$ ratio values of 1, 2, and 2, and $SO_4^{2-}/HCO_3^-{}_{meq/meq}$ values of 0, 0, and 1 (Liu and Han, 2020), respectively. In this study, most SW samples were close to the end members associated with carbonate weathering by H_2CO_3, while all GW samples were distributed among the three end members (H_2CO_3, HNO_3, and H_2SO_4) (Fig. 3c), demonstrating that the effects of HNO_3 and H_2SO_4 on hydrogeochemical evolution in GW were more significant compared to those in SW. Additionally, the involvement of HNO_3 and H_2SO_4 in carbonate weathering can result in increases in Ca^{2+}, Mg^2, NO_3^-, and SO_4^{2-} concentrations (Xie et al., 2021). It is seen from Fig. 3d that an obvious positive relationship between $NO_3^-+SO_4^{2-}$ and $Ca^{2+}+Mg^{2+}$ ($R^2 = 0.99$) in GW samples, suggesting the involvement of HNO_3 and H_2SO_4 in $Ca_xMg_{1-x}CO_3$ dissolution in GW. In contrast, these processes contributed little to Ca^{2+} and Mg^{2+} in SW due to the low NO_3^- and SO_4^{2-} concentrations.

4.2.2. $\delta^{13}C_{DIC}$ indicator

Previous studies have pointed out the deterioration of rainwater in Guilin City as a result of acid pollutants in the atmosphere, showing a mean pH value of rainwater below 5.5 (Yu et al., 2015; Li et al., 2020). Therefore, atmospheric CO_2 has a limited effect on karst water DIC (Huang et al., 2017). In this study, the mean partial pressure values of CO_2 (pCO_2) in SW and GW were 8044 ± 2486 and 9584 ± 3943 ppmv, respectively, which were 13–43 times higher than that in the atmosphere (~414 ppmv, https://keelingcurve.ucsd.edu/), suggesting a negligible contribution to karst water DIC. Therefore, karst water DIC was assumed to be derived from the soil CO_2 and the dissolution of calcite and dolomite minerals (Xie et al., 2021).

Theoretically, the more DIC originated from soil CO_2 results in a lower $\delta^{13}C_{DIC}$ value in karst water, thereby providing isotopic fingerprint evidence for understanding the carbonate weathering by different acids. The soil CO_2 is generally controlled by organic matter mineralization and soil respiration (Rasse et al., 2001; Polsenaere et al., 2013). Therefore, the $\delta^{13}C_{DIC}$ value of biogenic CO_2 is considered to be close to

that of organic matter in karst regions (Huang et al., 2017). The most identified local vegetations were C_3-type plants, while the $\delta^{13}C$ values of soil CO_2 ranged from − 26 to − 24‰, with a mean value of − 25‰ (Li et al., 2008). On the other hand, the $\delta^{13}C$ values of continental carbonate derived from marine rocks ranged from − 3 to + 2‰, with a mean value close to 0 (Clark and Fritz, 1997; Pan et al., 2002). The amount of soil CO_2 may generally decrease when carbonates are dissolved mainly by H_2CO_3 in a closed system. Theoretically, the $\delta^{13}C_{DIC}$ value may, therefore, be − 12.5‰ (i.e., (−25‰ + 0) × 0.5) in this study. However, the $\delta^{13}C_{DIC}$ levels in most karst water samples were higher than the expected value (Fig. 4), indicating that HNO_3 and H_2SO_4 were involved in carbonate weathering (Huang et al., 2017). Moreover, most water samples were close to the equilibrium dissolution end member of $Ca_xMg_{1-x}CO_3$, implying that chemical weathering could be dominated by thermodynamic control rather than kinetic control. The lowest $\delta^{13}C_{DIC}$ value (−13.79‰) was observed at GW04 and was assumed to represent the $\delta^{13}C_{DIC}$ value related to carbonate dissolution by H_2CO_3 in this study (Fig. 4), as the corresponding $[Ca^{2+}+Mg^{2+}]/[HCO_3^-]_{meq/meq}$ ratio value of 1.02 was close the theoretical $[Ca^{2+}+Mg^{2+}]/[HCO_3^-]_{meq/meq}$ ratio value of 1 (Xie et al., 2021). Indeed, relatively more $Ca_xMg_{1-x}CO_3$ and less soil CO_2 may be involved in the carbonate mineral dissolution processes when carbonate minerals are dissolved by H_2CO_3 together with HNO_3 and/or H_2SO_4, resulting in a relatively high $\delta^{13}C_{DIC}$ and $[Ca^{2+}+Mg^{2+}]/[HCO_3^-]_{meq/meq}$ values over − 13.79‰ and 1, respectively. Most GW samples with $\delta^{13}C_{DIC}$ values more than − 13.79‰ were collected from zones where carbonate minerals were dissolved by the combination of the three acids (Fig. 4), further indicating that besides H_2CO_3, HNO_3 and H_2SO_4 play a key role in carbonate weathering in the HKW.

4.3. Anthropogenic source of HNO_3

The microbial nitrification was the primary process affecting karst water NO_3^- in the HKW (Li et al., 2023), indicating the transformation of NH_4^+ to an oxidized form produces H^+ and NO_3^- ($NH_4^+ + 2O_2 \rightarrow NO_3^- + 2H^+ + H_2O$, Eq. (21); Zhang et al., 2020). Hence, estimating NO_3^- sources is a key step in HNO_3 quantification in karst water. The contribution of anthropogenic pollution sources to NO_3^- concentrations in the karst water of the HKW was reported in details by Li et al. (2022). In short, the NHF and SN were the major pollution sources of GW NO_3^- in the agricultural karst wetland (Fig. 5a). Furthermore, some sample points were plotted close to the NOF and MS zones and far from the AD zone, suggesting that karst water NO_3^- was also derived from NOF and MS rather than AD. However, not all samples were in a specific region of potential NO_3^- pollution, reflecting a mixture of pollution sources. In addition, Generally, the nitrogen pollution dynamics in GW are affected by the characteristics of the vadose zone (Niu et al., 2022). The well-developed karst of the HKW is characterized by a higher permeable aquifer and thinner soil layer, leading to rapid circulation of karst water and (Li et al., 2022), consequently, significantly reducing the residence time of NO_3^- in the vadose zone. Therefore, modern agricultural inputs (i.e., NHF) were identified as the main pollution sources of GW NO_3^- in the HKW.

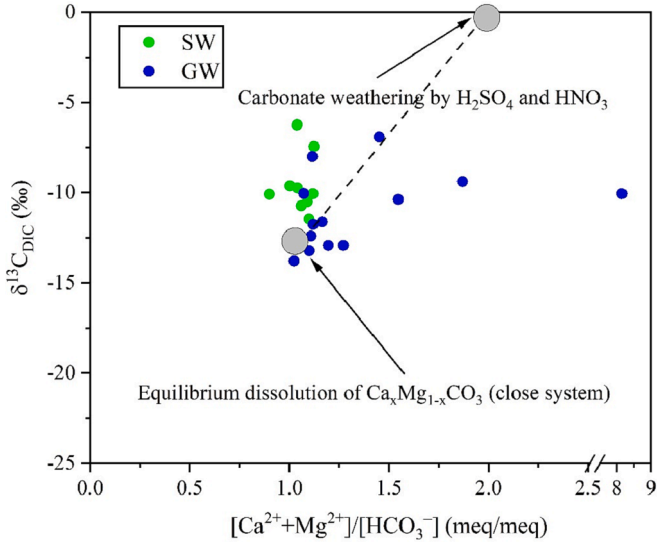

Fig. 4. Diagram of $\delta^{13}C_{DIC}$ and $[Ca^{2+}+Mg^{2+}]/[HCO_3^-]$ in SW and GW of the HKW.

The MixSIAR model was used in the present study to determine the contribution ratios of NO_3^- pollution sources. The obtained results are shown in Fig. 5b and Fig. S2. According to the obtained results, the primary pollution sources of karst water in the HKW were NHF (36.6%) and SN (28.0%), accounting for 64.6% of the total NO_3^- pollution sources, followed, respectively, by NOF (16.8%), MS (15.1%), and AD (3.44%). Furthermore, the results of the MixSIAR model were consistent with those obtained using the measured NO_3^- isotopes combined with the particular value ranges. Hence, according to the Eq. (11), the conversion coefficients between HNO_3 and NO_3^- in all samples could be determined (Table S3).

4.4. Anthropogenic sources of H_2SO_4

According to previous study (Xie et al., 2021), SO_4^{2-} in karst water generally originated from the geological background, anthropogenic inputs, and atmospheric deposition. However, sulfide minerals were almost not found in the HKW, which is consistent with the findings of the previous study in Guilin (Sun et al., 2021). The NHF, NOF, and synthetic potassium fertilizers are commonly applied to vegetable and fruit crop fields in the study area, while synthetic sulfur fertilizers are rarely applied by local farmers. Therefore, the contribution of geological background and synthetic fertilizers to karst water SO_4^{2-} was neglected in this study. However, the waste residue of pyrite is distributed in the northern part of the HKW, resulting in significant increases in SO_4^{2-} concentrations in the surrounding sampling sites (e.g., GW12, GW08, GW11, and GW02), which were 5–66 times higher than those observed at other sampling points. The pyrite oxidation might produce H^+ and SO_4^{2-} ($2FeS_2 + 7O_2 + 2H_2O \rightarrow 2FeSO_4 + 4H^+ + 2SO_4^{2-}$, Eq. (22); Xu et al., 2021), thereby participating in carbonate weathering in the HKW. Therefore, the waste pyrite residue is a primary pollution source of GW H_2SO_4 in the northern part of the HKW. Moreover, the H_2SO_4 in rainwater is primarily derived from a chemical reaction between SO_2 from fossil fuel combustion and free radicals in the atmosphere (e.g., OH, H_2O_2; Berner and Berner, 1987). In Guilin City, SO_4^{2-} concentration in precipitation ranged from 1.92 to 12.3 mg/L, which was identified as the most important acid-forming anion inducing acid rain (Yu et al., 2015; Li et al., 2020). The SO_4^{2-} concentrations in all SW samples and approximately 38.46% of GW samples were within this value range (Table 1), indicating that acid rain is also the main pollution source in the HKW. Therefore, H_2SO_4 in karst water was mainly derived from pyrite oxidation and acid rain in the HKW.

4.5. Influence of anthropogenic HNO_3 and H_2SO_4 on carbonate weathering and CO_2 sink

4.5.1. Carbonate weathering

The 20.91% and 21.69% in GW from HNO_3 and H_2SO_4 are the amazing contribution to carbonate weathering (Table S1), suggesting that natural processes of carbonate dissolution were seriously affected by anthropogenic pollution inputs derived from agricultural and mining activities in the HKW. It is noted that HNO_3 and H_2SO_4 can result in faster carbonate dissolution rates than H_2CO_3, thereby owning a priority in chemical weathering processes. As a result, HNO_3 and H_2SO_4 can obviously accelerate the dissolution rate of carbonate and promote the

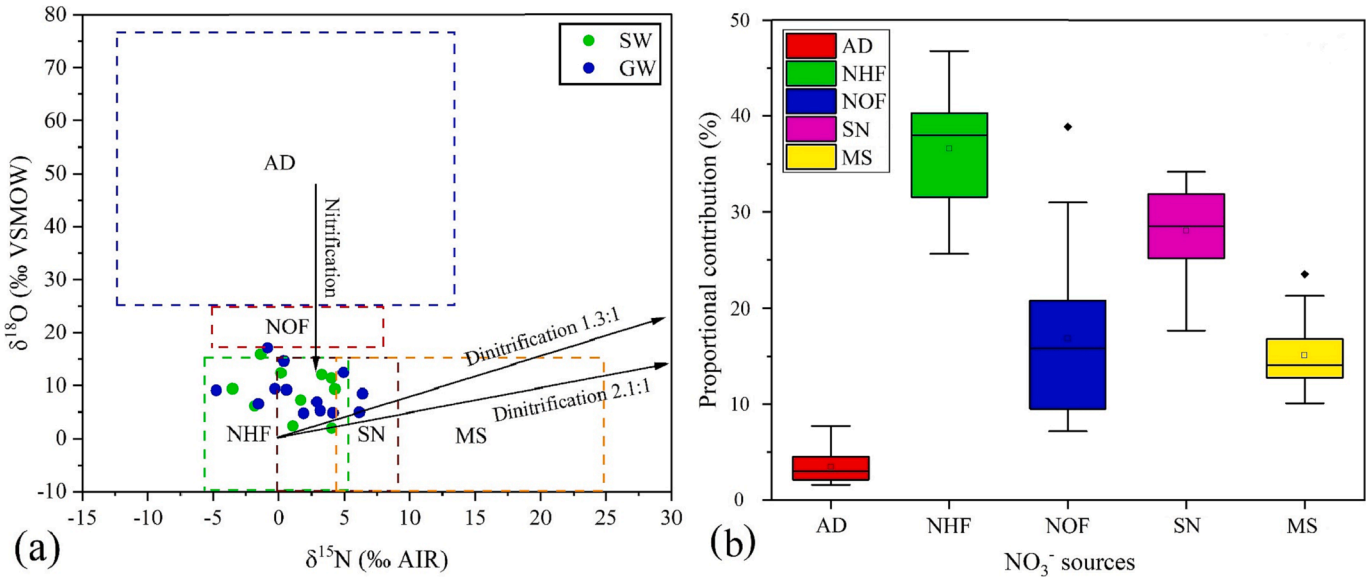

Fig. 5. Main pollution sources of karst water NO_3^- evaluated by the plots of (a) $\delta^{15}N\text{-}NO_3^-$ versus $\delta^{18}O\text{-}NO_3^-$ and (b) MixSIAR model (modified after Li et al., 2022).

aging of karst development (Waele et al., 2016), providing a favorable condition for shallow karst water to flow into deep karst aquifers and further dissolve deep carbonate minerals (Fig. 6a).

Generally, the over-exploitation of karst water resources leads to a decrease in ecological water levels, thereby resulting in karst water shortages. Obviously, in this study, anthropogenic HNO_3 and H_2SO_4 has increased carbonate weathering by a non-negligible contribution rate (42.60%; Fig. 6b), which were most likely to promote karst development, associated with a faster dissolution rate compared with H_2CO_3 in the HKW. Consequently, the same amount of recharge water is accompanied by the presence of considerable storage spaces in karst aquifers, resulting in low ecological water levels. Therefore, carbonate weathering by anthropogenic acids may be also an important cause of a decrease in ecological water levels, resulting in the shortage of karst water resource and degradation of wetland ecosystem.

4.5.2. CO_2 sink

The mean OP_{CO2} value in GW was as high as 42.60 ± 30.24% (Table S1), indicating that the involvement of anthropogenic acids in chemical weathering significantly decreased the CO_2 sink flux in the HKW. Changes in atmospheric and soil CO_2 not only affect carbonate weathering in karst regions but are also related to global climate change (Berner et al., 1983; Kump et al., 2000; Berner, 2003). CO_2, as the third most important greenhouse gas, can trap heat in the atmosphere and, consequently, increase global temperature through the greenhouse effect. In the context of global climate warming, future climate change depends on the emission and absorption of greenhouse gas to a certain extent. Indeed, previous studies have devoted considerable attention to CO_2 emissions from industrial activities since the Industrial Revolution (Falkowski, et al., 2000), while this study focused mainly on the natural process of CO_2 absorption disturbed by anthropogenic activities in karst wetland areas. The impacts of anthropogenic acids on the earth's surface

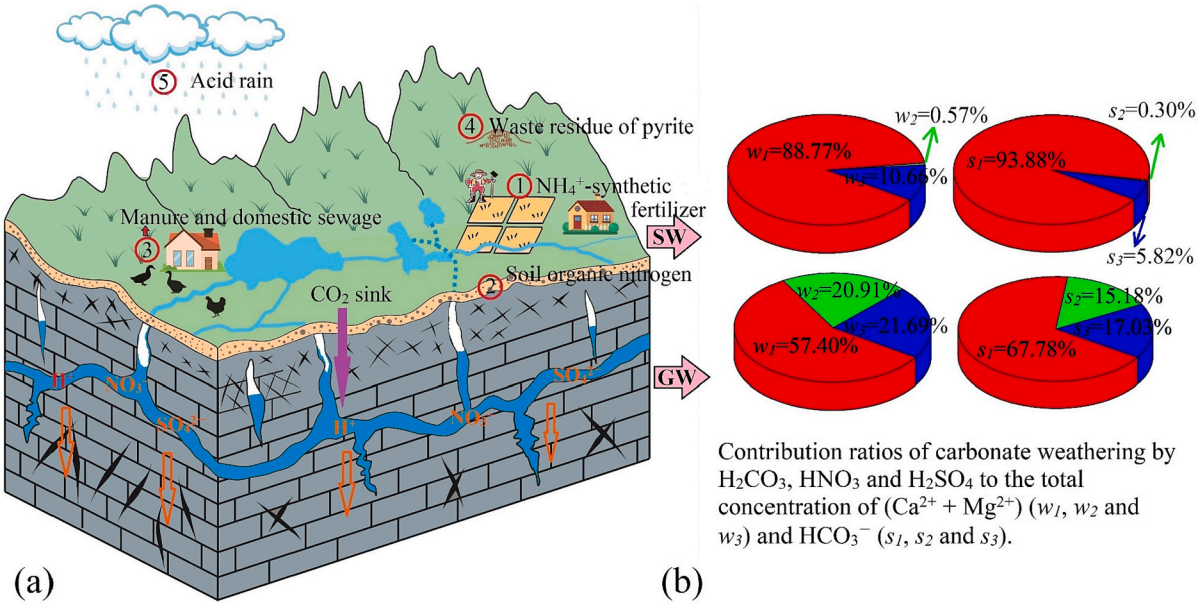

Fig. 6. (a) Conceptual model of carbonate rocks dissolved by anthropogenic HNO_3 and H_2SO_4; (b) Proportional contribution of H_2CO_3, HNO_3 and H_2SO_4 to carbonate weathering in the HKW.

C cycle have been investigated in different regions worldwide (Calmels et al., 2014; Gulley et al., 2016; Waele et al., 2016; Zhao et al., 2021). Moreover, carbonate minerals constitute the earth's largest C reservoir (Martin, 2017). Therefore, considerable attention needs to be devoted to the impact of carbonate weathering on the karst C cycle and global climate change.

4.6. Ecological environmental management implications

Generally, healthy karst wetland ecosystems depend on adequate water resources. In previous study, the excessive consumption of water resources and biological resources by human activities has led to a decrease in karst groundwater levels and the degradation of wetland ecosystem in the HKW, including reduction of wetland area and biodiversity (Zou et al., 2019). Although some water replenishment measures have been implemented in the HKW to restore the wetland ecosystem, a decrease in ecological water levels caused by anthropogenic acids from agricultural and mining activities is still ignored. The obtained results in this study provide further insights into the development of a more reasonable ecological restoration plan based on karst water resource regulation and management, focusing on the control of acidic pollutant discharges as follows:

(i) Establishing optimal fertilization plans to improve the utilization of NH_4^+-synthetic fertilizers and avoid overuse of NH_4^+-synthetic fertilizers, such as precise fertilization of root soils, application of slow-synthetic fertilizers, and addition of nitrogen fertilizer synergists (Li et al., 2023);

(ii) Taking effective seepage control measures to prevent karst groundwater from the leachate of waste pyrite residue, for instance, the coverage of waterproof material at the surface of waste pyrite residue combing with drainage channels, and construction of impervious layer at the bottom;

(iii) Strengthening the management and supervision of acid pollutants discharge and improving the public awareness of environmental protection in the HKW.

5. Conclusions

In this study, the hydrogeochemical and isotopic ($\delta^{15}N\text{-}NO_3^-$, $\delta^{18}O\text{-}NO_3^-$ and $\delta^{13}C_{DIC}$) analyses combined with the MixSIAR model and stoichiometric coefficients was an effective method for estimating the proportional contributions of H_2CO_3, HNO_3, and H_2SO_4 to carbonate weathering and the CO_2 sink in the HKW. According to obtained hydrogeochemical compositions and $\delta^{13}C_{DIC}$ values, the karst hydrogeochemical processes in the HKW were mainly controlled by carbonate weathering, which is not only induced by H_2CO_3 but also by HNO_3 and H_2SO_4 with non-negligible contributions, especially in GW. The results obtained from the MixSIAR model and stoichiometric coefficients showed that the contribution rates of HNO_3 and H_2SO_4 to carbonate weathering were 20.91 ± 19.29 and 21.69 ± 26.88% in GW, and 0.57 ± 0.72 and 10.66 ± 8.02% in SW respectively. Thus, the chemical weathering rates were accelerated by anthropogenic HNO_3 and H_2SO_4 in GW. The corresponding overestimated proportions of CO_2 sink were 11.23 ± 7.94 and 42.60 ± 30.24% in SW and GW, respectively, suggesting that the involvement of anthropogenic acids in chemical weathering significantly decreased the CO_2 sink flux. It is noted that the anthropogenic HNO_3 and H_2SO_4 involved in carbonate weathering not only affect the karst C cycle and global climate change, but also accelerate the chemical weathering rates, which is an important reason for a decrease in ecological water levels besides the over-exploitation in the HKW. Therefore, the contribution of anthropogenic acids to carbonate weathering should not be ignored in the restoration of wetland ecosystems.

Declaration of Competing Interest

The authors declare that they have no known competing financial interests or personal relationships that could have appeared to influence the work reported in this paper.

Data availability

Data will be made available on request.

Acknowledgements

This study was supported by the Foundation for Hebei Education Department (2022QNJS05 and QN2020424), China Geological Survey Project (DD20221758), and Natural Scientific Foundation of Guangxi Zhuang Autonomous Region (2021GXNSFBA220065). Special thanks to research assistant professor Hengxing Zhang, who serves as the Institute of Hydrogeology and Environmental Geology, Chinese Academy of Geological Sciences, He provided the great supports during the manuscript revision process.

Appendix A. Supplementary data

Supplementary data to this article can be found online at https://doi.org/10.1016/j.ecolind.2023.110192.

References

Berner, R.A., 2003. The long-term carbon cycle, fossil fuels and atmospheric composition. Nature 426 (6964), 323–326.
Berner, E.K., Berner, R.A., 1987. The Global Water Cycle: Geochemistry and Environment. Prentice-Hall, New York, p. 394.
Berner, R.A., Kothavala, Z., 2001. Geocarb III: a revised model of atmospheric CO2 over Phanerozoic Time. Am. J. Sci. 301 (2), 182–204.
Berner, R.A., Lasaga, A.C., Garrels, R.M., 1983. The carbonate-silicate geochemical cycle and its effect on atmospheric carbon dioxide over the past 100 million years. Am. J. Sci. 283 (7), 641–683.
Calmels, D., Gaillardet, J., François, L., 2014. Sensitivity of carbonate weathering to soil CO_2 production by biological activity along a temperate climate transect. Chem. Geol. 390, 74–86.
Cartwright, I., 2010. The origins and behaviour of carbon in a major semiarid river, the Murray River, Australia, as constrained by carbon isotopes and hydrochemistry. Appl. Geochem. 25, 1734–1745.
Clark, I.D., Fritz, P., 1997. Environmental Isotopes in Hydrogeology. Lewis Publishers, New York.
Falkowski, P., Scholes, R.J., Boyle, E., et al., 2000. The global carbon cycle: A test of our knowledge of earth as a system. Science 290 (5490), 291–296.
Gulley, J., Martin, J., Brown, A., 2016. Organic carbon inputs, common ions and degassing: rethinking mixing dissolution in coastal eogenetic carbonate aquifers. Earth Surf. Process. Landf. 41, 2098–2110.
Han, G.L., Tang, Y., Wu, Q.X., 2010. Hydrogeochemistry and dissolved inorganic carbon isotopic composition on karst groundwater in Maolan, southwest China. Environ. Earth Sci. 60 (4), 893–899.
Huang, Q., Qin, X., Liu, P., Zhang, L., Su, C., 2017. Impact of sulfuric and nitric acids on carbonate dissolution, and the associated deficit of CO_2 uptake in the upper–middle reaches of the Wujiang River. China. J. Contam. Hydrol. 203, 18–27.
Huang, F., Xiao, Q., Yin, W., Hu, G., Yang, L., Liu, Z., Cao, J., 2014. The effects of using N-fertilizers in soil on karst carbon sink in karst system. Carsologica Sinica. 33 (4), 405–411.
Jiang, Y., 2013. The contribution of human activities to dissolved inorganic carbon fluxes in a karst underground river system: Evidence from major elements and $\delta^{13}C_{DIC}$ in Nandong, Southwest China. J. Contam. Hydrol. 152, 1–11.
Kump, L.R., Brantley, S.L., Arthur, M.A., 2000. Chemical weathering, atmospheric CO2, and climate. Annu. Rev. Earth Planet. Sci. 28, 611–667.
Li, S.L., Calmels, D., Han, G., Gaillardet, J., Liu, C.Q., 2008. Sulfuric acid as an agent of carbonate weathering constrained by delta C-13(DIC): examples from Southwest China. Earth Planet. Sci. Lett. 270 (3–4), 189–199.
Li, L., Li, H., Peng, L., Li, Y., Zhou, Y., Chai, F., Mo, Z., Chen, Z., Mao, J., Wang, W., 2020. Characterization of precipitation in the background of atmospheric pollutants reduction in Guilin: Temporal variation and source apportionment. J. Environ. Sci. 98, 1–13.
Li, J., Zou, S., Zhao, Y., Zhao, R., Dang, Z., Pan, M., Zhu, D., Zhou, C., 2021. Major ionic characteristics and factors of karst groundwater at Huixian karst wetland. China. Environ. Sci. 42 (4), 1750–1760.
Li, J., Zhu, D., Zhang, S., Yang, G., Zhao, Y., Zhou, C., Lin, Y., Zou, S., 2022. Application of the hydrochemistry, stable isotopes and MixSIAR model to identify nitrate sources

and transformations in surface water and groundwater of an intensive agricultural karst wetland in Guilin. China. Ecotox. Environ. Safe. 231, 113205.
Li, J., Zou, S., Wang, J., Zhou, C., Wu, Y., Zhang, H., Zhao, Y., Yang, G., 2023. Spatiotemporal variability and control factors of NO_3^- in a polluted karst water system of an agricultural wetland in South China. Chemosphere 313, 137435.
Liu, Z.H., 2012. New progress and prospects in the study of rock-weathering-related carbon sinks. Chin. Sci. Bull. (Chin. Ver.) 57, 95–102.
Liu, J., Han, G., 2020. Effects of chemical weathering and CO_2 outgassing on $\delta^{13}C_{DIC}$ signals in a karst watershed. J. Hydrol. 589, 125192.
Martin, J.B., 2017. Carbonate minerals in the global carbon cycle. Chem. Geol. 449, 58–72.
Niu, X., Jia, X., Yang, X., Wang, J., Wei, X., Wu, L., Shao, M., 2022. Tracing the sources and fate of NO_3^- in the vadose zone−groundwater system of a thousand-year-cultivated region. Environ. Sci. Technol. 56, 9335–9345.
Pan, G., He, S., Cao, J., Tao, Y., Sun, Y., 2002. Varistion of $\delta^{13}C$ in karst soil in Yaji Karst Experiment Site. Guilin. Chinese Sci. Bull. 47, 500–503.
Perrin, A., Probst, A., Probst, J., 2008. Impact of nitrogenous fertilizers on carbonate dissolution in small agricultural catchments: Implications for weathering CO2 uptake at regional and global scales. Geochim. Cosmochim. Ac. 72 (13), 3105–3123.
Polsenaere, P., Savoye, N., Etcheber, H., Canton, M., Poirier, D., Bouillon, S., Abril, G., 2013. Export and degassing of terrestrial carbon through watercourses draining a temperate podzolized catchment. Aquat. Sci. 75 (2), 299–319.
Rasse, D.P., François, L.M., Aubinet, M., Kowalski, A.S., Walle, I.V., Laitat, E., Gérard, J. C., 2001. Modelling short-term CO2 fluxes and long-term growth in temperate forests with ASPECTS. Ecol. Model. 141, 35–52.
Raymond, P.A., Oh, N.H., Turner, R.E., Broussard, W., 2008. Anthropogenically enhanced fluxes of water and carbon from the Mississippi River. Nature 451 (7177), 449–452.
Ren, K., Pan, X., Yuan, D., Zeng, J., Liang, J., Peng, C., 2022. Nitrate sources and nitrogen dynamics in a karst aquifer with mixed nitrogen inputs (Southwest China): Revealed by multiple stable isotopic and hydro-chemical proxies. Water Res. 210, 118000.
Silva, S.R., Kendall, C., Wilkison, D.H., Ziegler, A.C., Chang, C.C.Y., Avanzino, R.J., 2000. A new method for collection of nitrate from fresh water and the analysis of nitrogen and oxygen isotope ratios. J. Hydrol. 228 (1), 22–36.
Standardization Administration, 2017. Standard for Groundwater Quality (GB/T14848–2017).
Sun, P., He, S., Yu, S., Pu, J., Yuan, Y., Zhang, C., 2021. Dynamics in riverine inorganic and organic carbon based on carbonate weathering coupled with aquatic photosynthesis in a karst catchment. Southwest China. Water Res. 189, 116658.
Wachniew, P., 2006. Isotopic composition of dissolved inorganic carbon in a large polluted river: the Vistula. Poland. Chem. Geol. 233 (3–4), 293–308.
Waele, J.D., Audra, P., Madonia, G., Vattano, M., Plan, L., D'Angeli, I.M., Bigot, J.Y., Nobécourt, J.C., 2016. Sulfuric acid speleogenesis (SAS) close to the water table: Examples from southern France, Austria, and Sicily. Geomorphology 253, 452–467.
Xie, Y., Huang, F., Yang, H., Yu, S., 2021. Role of anthropogenic sulfuric and nitric acids in carbonate weathering and associated carbon sink budget in a karst catchment (Guohua), southwestern China. J. Hydrol. 599, 126287.
Xu, S., Li, S., Su, J., Yue, F., Zhong, J., Chen, S., 2021. Oxidation of pyrite and reducing nitrogen fertilizer enhanced the carbon cycle by driving terrestrial chemical weathering. Sci. Total Environ. 768, 144343.
Xue, D., Botte, J., Baets, B.D., Accoe, F., Nestler, A., Taylor, P., Cleeput, O.V., Berglund, M., Boeckx, P., 2009. Present limitations and future prospects of stable isotope methods for nitrate source identification in surface- and groundwater. Water Res. 43, 1159–1170.
Yu, S., Kuo, Y.M., Du, W., He, S., Sun, P.A., Yuan, Y., Li, R., Li, Y., 2015. The hydrochemistry properties of precipitation in karst tourism city (Guilin). Southwest China. Environ. Earth Sci. 74, 1061–1069.
Zeng, J., Han, G., Wu, Q., Tang, Y., 2020. Effects of agricultural alkaline substances on reducing the rainwater acidification: insight from chemical compositions and calcium isotopes in a karst forests area. Agric. Ecosyst. Environ. 290, 106782.
Zhang, Y., Jiang, Y., Yuan, D., Cui, J., Li, Y., Yang, J., Cao, M., 2020. Source and flux of anthropogenically enhanced dissolved inorganic carbon: A comparative study of urban and forest karst catchments in Southwest China. Sci. Total Environ. 725, 138255.
Zhao, R., Liu, Z., Dong, L., Zhang, Q., Liu, C., 2021. The fates of CO_2 generated by H_2SO_4 and/or HNO_3 during the dissolution of carbonate and their influences on the karst-related carbon cycle. J. Hydrol. 597, 125746.
Zou, S., Zhou, C., Zhu, D., Lin, Y., Fan, L., Xie, H., Wang, J., Li, J., 2019. Scientific protection of Huixian karst wetland in Guilin. China Mining Magazine, 2019, 28(S1): 353–357.